Effects of retigabine and the novel M-current activator BHV-7000 on epilepsy-associated *KCNQ2* variants

[1]Carlos G. Vanoye, [1]Reshma R. Desai, [1]Nora F Ghabra, [1]Alexandra E. Hong, [2]Kelly Picchione, [2]Steven Dworetzky and [1]Alfred L. George, Jr.

[1]Department of Pharmacology, Northwestern University Feinberg School of Medicine, Chicago, IL; [2]Biohaven, LTD, New Haven, CT

ABSTRACT

Rationale: The voltage-gated potassium channels KCNQ2 (K_V7.2; Q2) and KCNQ3 (K_V7.3; Q3), encoded by *KCNQ2* and *KCNQ3*, respectively, co-assemble to form a channel complex (Q2/Q3) responsible for generating the M-current that regulates neuronal excitability. *KCNQ2* pathogenic variants identified in children with developmental and epileptic encephalopathy (DEE) most often exhibit loss-of-function with dominant-negative effects. Pharmacological potentiation of M-current with retigabine (RET) or newer investigational agents such as BVH-7000 (BHV; formally KB-3061) is a potential therapy for this condition. Here, we compared the effects of RET with BHV on wild-type (WT) Q2/Q3 and channels comprised of DEE-associated *KCNQ2* variants.

Methods: We expressed Q2/Q3 channels in Chinese hamster ovary (CHO) cells and recorded whole-cell currents using automated planar patch clamp first in the absence then presence of vehicle (DMSO) or M-current activator (RET or BVH). Experiments were conducted using cells transfected with an equal mixture of WT and variant KCNQ2 along with WT KCNQ3 to generate heteromultimeric channel complexes that recapitulated the heterozygous state. Specific channel activity was determined by applying the M-current blocker XE-991 (10 µM) at the end of experiments, and only XE-991-sensitive currents were analyzed.

Results: At 3 µM, both compounds induced significant hyperpolarizing shifts in the voltage-dependence of activation (delta V½) of WT channels, but the effect was greater for BHV (RET = -18.7±1.7, n=13; BHV = -32.1±1.4, n=8). Both compounds boosted current amplitude to a similar degree (relative to the no drug condition: RET = 7.0±0.9 fold increase; BHV = 6.2±0.9 fold increase) when measured during -10 mV test pulses. The half-maximal effective concentration (EC_{50}) for delta V½ of WT channels were RET = 4.9 µM; BHV = 1.4 µM. We also assessed the effects of RET and BHV on channels incorporating KCNQ2 variants for which clinical responses to retigabine treatment were reported. BVH (3 µM) induced greater hyperpolarizing shifts in activation V½ than RET (3 µM).

Conclusions: The M-current activators RET and BHV exhibited effects on WT Q2/Q3 channels and restored current for channels containing DEE-associated pathogenic *KCNQ2* variants. We are testing several additional variants and determining concentration-response relationships for a more complete understanding of these effects. Delineating the heterogeneity of M-current activator responsiveness of pathogenic variants may enable better deployment of precision pharmacotherapies for KCNQ2-DEE.

Background

KCNQ2 pathogenic variants identified in children with developmental and epileptic encephalopathy (DEE) most often exhibit loss-of-function with dominant-negative effects. Pharmacological potentiation of M-current is a potential therapy for this condition. Our previous results (Vanoye et al,2022, JCI Insight) demonstrated genotype-dependent differences in the response of *KCNQ2* variants to retigabine, a proposed precision therapy for *KCNQ2* developmental and epileptic encephalopathy. In this study we investigated whether the newer investigational agent BVH-7000 (BHV; formally KB-3061) exhibits genotype-dependent differences.

Methods

-*Cell Culture*: Chinese hamster ovary cells (CHO-K1) stably expressing KCNQ3-WT (CHO-Q3) were grown in F-12 nutrient mixture medium supplemented with fetal bovine serum, penicillin and streptomycin with hygromycin selection at 37°C in 5% CO_2.

-*Molecular Biology*: Variants were introduced into human KCNQ2 using Quikchange mutagenesis (Agilent technologies). KCNQ2 variants were expressed from plasmid pIRES2_KCNQ2_EGFP, whereas KCNQ2-WT was expressed from plasmid pIRES2_KCNQ2_CyOFP. These plasmids included green or orange fluorescent proteins, respectively, as transfection markers. The KCNQ2 reading frame of all constructs was sequenced completely.

-*Electroporations*: Wild type plus KCNQ2 variant cDNAs were transiently co-transfected into CHO_KCNQ3 cells using the MaxCyte STX system.

-*Flow Cytometry*: Transfection efficiency was evaluated by flow cytometry (CytoFLEX, Beckman Coutler) using a 488 nm laser and filters for green fluorescence (FITC, KCNQ2_variants coupled to EGFP expression), and orange fluorescence (PEA, KCNQ2_WT couple to CyOFP expression).

-*Electrophysiology*: Automated planar patch clamp recording was performed on the Nanion SyncroPatch 768 PE platform. External solution contained (in mM): 140 NaCl, 4 KCl, 2.0 $CaCl_2$, 1 $MgCl_2$, 10 HEPES, 5 glucose, pH 7.4. The composition of the internal solution was (in mM): 60 KF, 50 KCl, 10 NaCl, 20 EGTA, 10 HEPES, 5 mM MgATP, pH 7.2. Retigabine (SIGMA) and BHV-7000 (Biohaven) were added from 10 mM stock solutions dissolved in DMSO. DMSO volume was constant for all compound concentrations (0-30 µM; 3 µl/ml). Whole-cell currents were recorded at room temperature from holding potential of -80 mV using 1000 ms depolarizing pulses from -80 to +40 mV (in 10 mV steps), followed by a 250 ms step to 0 mV to analyze tail currents. Number of cells (n) is given on the figure legends.

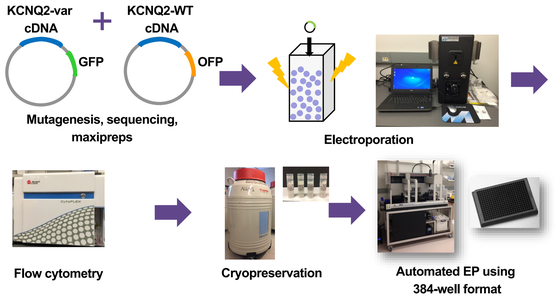

Fig. 1 – Experimental work-flow for high throughput functional studies of KCNQ2 variants expressed in CHO-K1 cells stably expressing human KCNQ3 (CHO-Q3 cells).

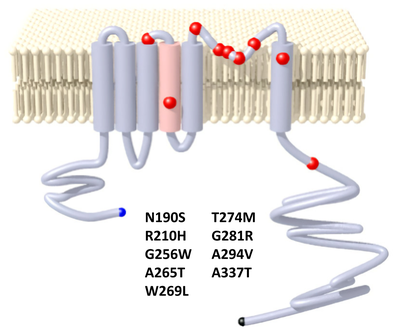

Fig. 2 – Variants analyzed in this study and location in the KCNQ2 protein.

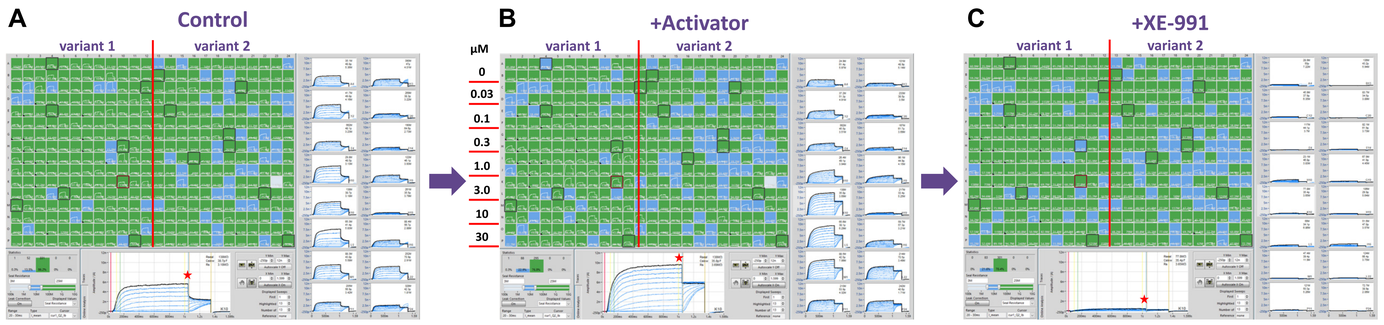

Fig. 3 Whole-cell recording protocol and use of XE-991 to isolate KCNQ2 + KCNQ3 current.

Screen-shots of whole-cell current recordings from CHO-Q3 cells transiently expressing KCNQ2 variants (2 variants, 12 columns per variant, 192 data points per variant) recorded under Control conditions **(A)**, following addition of 0-30 µM Activator (24 data points per concentration). **(B)**, and after the addition of 10 µM XE-991 **(C)** Currents recorded in the presence of XE-991 were digitally subtracted from the Control and +Activator data. Only the XE-991-sensitive currents were analyzed. Whole-cell currents were measured at the end (998 ms) of a 1000 ms long voltage step (★).

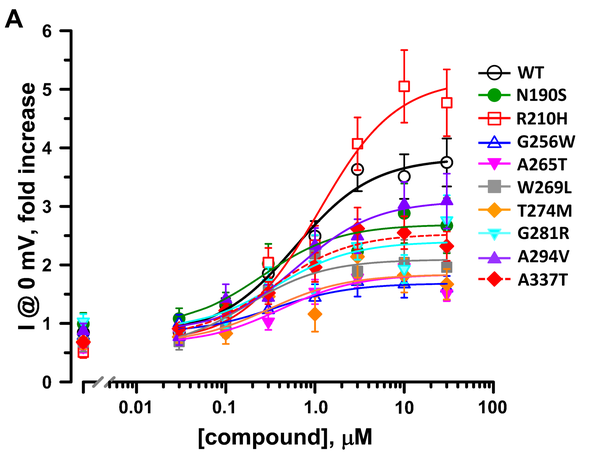

B

Channel variant	EC_{50}, µM	Maximum fold increase	Fold increase @ EC_{50}
WT	0.6 ± 0.2	3.8 ± 0.2	2.3
N198S	0.2 ± 0.2	2.7 ± 0.2	1.8
R210H	1.1 ± 0.4	5.2 ± 0.3	2.9
G256W	0.3 ± 0.3	1.7 ± 0.1	1.3
A265T	0.4 ± 0.2	1.8 ± 0.1	1.2
W269L	0.2 ± 0.1	2.1 ± 0.3	1.3
T274M	0.3 ± 0.3	1.8 ± 0.2	1.2
G281R	0.4 ± 0.3	2.4 ± 0.2	1.6
A294V	0.6 ± 0.4	3.1 ± 0.2	2.0
A337T	0.3 ± 0.2	2.5 ± 0.1	1.6

Fig. 4 – Concentration response for BHV-7000 induced changes in whole-cell current density recorded at 0 mV

A. Average concentration response curves obtained from KCNQ2 wild type and variants expressed as heterozygous channels (+KCNQ2-WT) exposed to various BHV-7000 concentrations. **B**. List of parameters from fitted data. N = 12-23 per concentration.

+Activator whole-cell currents were normalized to whole-cell currents recorded under Control conditions. Normalized data were fit with the equation ***Y = Bottom + X * (Top-Bottom)/ (EC_{50} + X)***.

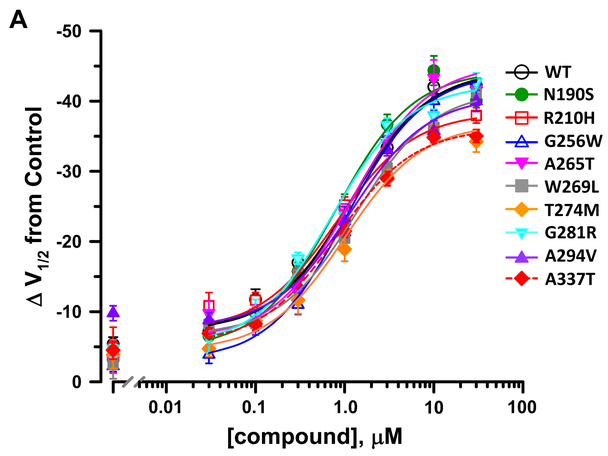

B

Channel variant	EC_{50}, µM	Max. ΔV½, mV	ΔV½ @ EC_{50}, mV
WT	1.2 ± 0.2	-44.4 ± 1.0	-25.9
N198S	0.8 ± 0.1	-44.4 ± 1.4	-24.1
R210H	0.8 ± 0.2	-38.4 ± 1.0	-22.8
G256W	1.1 ± 0.1	-44.1 ± 0.9	-23.6
A265T	1.2 ± 0.2	-45.3 ± 1.5	-25.6
W269L	1.3 ± 0.2	-41.5 ± 1.2	-24.0
T274M	1.0 ± 0.2	-36.9 ± 1.3	-20.6
G281R	0.7 ± 0.1	-42.5 ± 1.0	-23.8
A294V	1.2 ± 0.2	-40.7 ± 1.3	-24.2
A337T	0.8 ± 0.1	-36.2 ± 0.7	-20.8

Fig. 5 – Concentration response for BHV-7000 induced hyperpolarization of activation voltage-dependence

A. Average concentration response curves obtained from KCNQ2 wild type and variants expressed as heterozygous channels (+KCNQ2-WT) exposed to various BHV-7000 concentrations. **B**. List of parameters from fitted data. N = 6-20 per concentration.

Voltage-dependence of activation values under Control and +Activator conditions were derived from tail currents normalized to maximal tail current amplitude and expressed as a function of the preceding voltages. Data were fit to a Boltzmann function ***I(V) = Bottom + (Top-Bottom) / (1 + exp((V½ -V)/ slope))***.

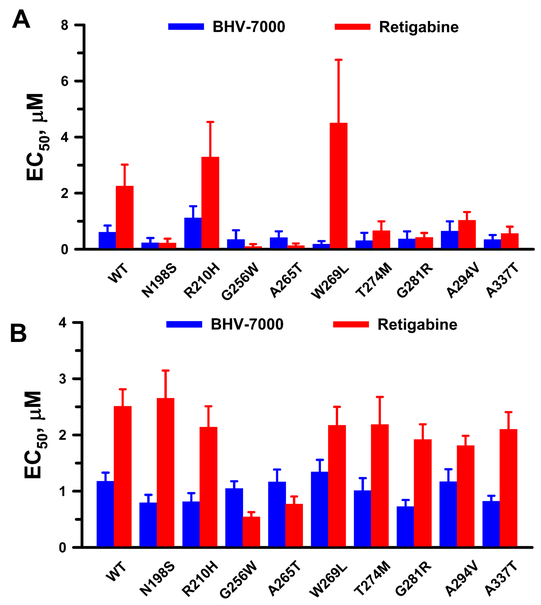

Fig. 6 – EC_{50} values calculated for (A) changes in current density recorded at 0 mV, and (B) activation V½.

EC_{50} values were derived from concentration response curves obtained from KCNQ2 wild type and variants channels expressed as heterozygous channels (+KCNQ2-WT) exposed to various BHV-7000 and retigabine concentrations. N = 5-23 per concentration.

Summary

1. Pharmacological potentiation of variant KCNQ2 channels expressed in the heterozygous state can be analyzed by automated patch clamp.
2. Automated patch clamp analysis of variant KCNQ2 channels reveal that KCNQ2 channels exhibit dissimilar responses to activator exposure.
3. EC_{50} values calculated for BHV-7000 and retigabine-induced increase in current density and hyperpolarization of the voltage-dependence of activation show larger heterogeneity for retigabine and more potent modulation for BHV-7000.

Conclusion

Pharmacological potentiation of pathogenic KCNQ2 channels is variant dependent. Further understanding of variant-specific responsiveness may enable better deployment of targeted therapies.

Supported by NIH grant U54-NS108874